

# Surface roughening and self-organized criticality: the influence of quenched disorder.

C. M. AEGERTER<sup>1</sup>, M. S. WELLING<sup>2</sup> and R. J. WIJNGAARDEN<sup>2</sup>

<sup>1</sup>*Fachbereich Physik, University of Konstanz, Universitatstrasse 10, 78457 Konstanz, Germany*

<sup>2</sup>*Division of Physics and Astronomy, Vrije Universiteit, De Boelelaan 1081, 1081HV Amsterdam, The Netherlands*

PACS. 05.65.+b – Self-organized systems.

PACS. 64.60.Ht – Dynamic critical phenomena.

PACS. 74.25.Qt – Vortex lattices, flux pinning, flux creep.

**Abstract.** – Self-organized criticality (SOC) has attracted considerable interest due to its possible wide ranging implications on broad range of subjects. However the experimental observation of SOC using stringent criteria has been difficult and the question of the critical parameters to observe SOC remains open. This is partly due to the fact that there are different criteria applied in order to claim SOC. Here we endeavour to study two aspects of this. First of all, we study the influence of the presence of quenched disorder on the appearance of SOC in the vortex dynamics in Niobium by changing the amount of Hydrogen impurities. Furthermore, we study whether the roughness properties of the pile surface can be used as a criterion for the appearance of SOC on par with the observation of finite size scaling. For this purpose, we compare the roughness and dynamic exponents of the vortex landscape to the avalanche size distribution for different amounts of disorder. The absence of a transition to SOC in the roughness exponent implies that the presence of a rough surface by itself cannot be used as a sufficient criterion for the observation of SOC. A determination of the dynamics of the surface properties however, shows a transition similar to that of the avalanche properties.

*Introduction.* – Self-organized criticality (SOC) [1] has attracted considerable interest due to its possibly wide ranging applicability in describing the natural world [2]. However on the side of stringent experimental observation, the situation is more complicated. This is in part due to the fact that for such investigations, one needs to have a model system, where all of the relevant parameters can be controlled and all of the relevant properties can be determined. In many cases this is difficult, and clear-cut, stringent criteria for SOC are usually not applied in experiments looking for SOC, but one simply studies the occurrence of power-laws in the avalanche distributions [3] or the surface roughness [4]. In order to show that a system indeed is in a critical state, there should however be a scaling of the properties with the system size (finite size scaling), which in addition yields information on other relevant exponents. A theoretical investigation of different SOC models [5] has found that there are a number of scaling relations between the different exponents in a SOC system. With a full

characterisation of many experimental parameters these can then be checked as well, providing an even more stringent test of SOC. Recently, such an investigation has been carried out on a three dimensional pile of rice, where both the avalanche size distribution for different system sizes and the surface roughness and dynamics were determined [6]. The applicable scaling relations [5] between these different quantities were fulfilled [6]. A similar investigation was carried out by studying magnetic vortices in  $\text{YBa}_2\text{Cu}_3\text{O}_7$  [7, 8], where the same parameters were checked and the same scaling relations were fulfilled. This finding has shown that there is an intimate connection between surface roughness and SOC as exemplified by the scaling relations. On the other hand, many systems which were thought to exhibit SOC from a modeling point of view, such as fine powders in a rotating drum, or piles of sand grown on a flat plate from a point source, have *not* faced up with experimental tests of SOC [9]. Thus it was unclear what critical parameters had to be applied in order to observe SOC. From investigations of a one-dimensional pile of rice [10] and a two dimensional pile of beads [11], where finite size scaling of the avalanches was observed, the role of slow driving and over-damped dynamics was emphasized. This is also corroborated in theory, where in the view of SOC as a phase transition [12], slow driving is *the* necessary parameter to reach an underlying critical point. On the other hand, Altshuler *et al.* [13] have studied a one dimensional pile of steel balls with different types of bases and found that only with rough bases was there finite size scaling of the avalanches and hence SOC. This has lead to the conjecture that the presence of quenched disorder is a necessary prerequisite in order to observe SOC [13]. Again, this is firmly based in theory as many SOC models can be mapped to percolation type phase transitions, which depend crucially on the presence of quenched disorder [12, 14–16].

In the critical state in type II superconductors, SOC was observed by many authors using various criteria [3, 4, 7, 17]. When magnetic vortices enter a sample, the competition of Lorentz and pinning forces leads to the build-up of a constant flux gradient [18]. In fact, the problem can be mapped onto that of a growing pile of sand [19], where the vortices take the role of the grains and the flux jumps that of the avalanches. The observation of SOC in flux avalanches has mainly relied on the presence of strong pinning in the samples, illustrating the importance of quenched disorder for the observation of SOC. We have previously studied the effect of quenched disorder quantitatively by varying its amount in the superconductor Nb by introducing H impurities [17]. By studying the avalanche size distributions with different cut-off sizes, we found that a minimum amount of quenched disorder is necessary in order to produce a finite size scaling collapse of the avalanche size distributions and hence a critical state. Here, we study the roughness properties of the corresponding flux landscapes in order to determine to what extent such roughness properties can be used as an indicator for the occurrence of SOC as is indicated by the presence of scaling relations [5]. For this purpose we determine the spatio-temporal correlation functions of the flux landscape and their roughness and growth exponents [20] for different amounts of quenched disorder. Their dependence on the amount of disorder is compared to the observation of finite size scaling [17].

*Experimental setup.* – The experiments were carried out in an advanced magneto-optical (MO) microscope [21] capable of determining directly the magnetic flux density,  $B_z$ , at the surface of the sample. The sample is placed underneath an Yttrium-Iron Garnet indicator [22], which has a mirror layer on its bottom. In contrast to more usual MO setups, the incoming polarisation is modulated by a certain angle  $\alpha$  in our apparatus [21]. Thus we have an increased resolution at small magnetic flux densities which is important in determining the size and distribution of flux avalanches in our samples. The spatial distribution of magnetic flux density is recorded using a charged coupled device (CCD) camera with a resolution of  $782 \times 582$  pixels, resulting in a spatial resolution of  $3.4 \mu\text{m}$  on the sample.

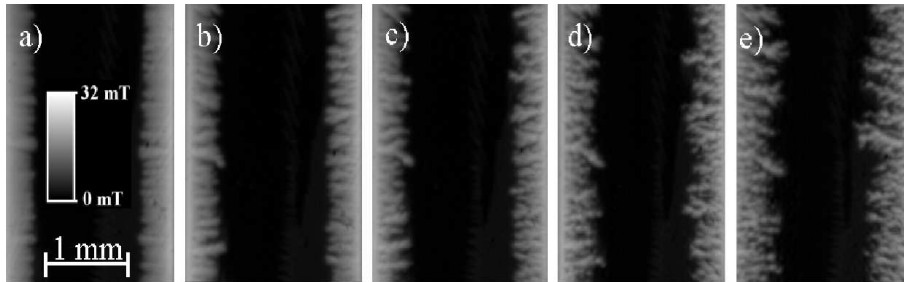


Fig. 1 – The magnetic flux landscape as determined by MO imaging for different H loading pressures. The values of the local flux densities are indicated by the scale bar in a), which applies to all figures. Part a) shows the as deposited film, whereas parts b)-e) show increasing H loading pressures of 80, 260, 1130, 1810 Pa respectively. As can be seen from the figure, the flux landscapes change drastically becoming much more rugged and less compact with increasing H impurities.

The samples consist of Nb films of a thickness of 500 nm, which were deposited under ultra high vacuum conditions onto a sapphire substrate in its R-plane ( $1\bar{1}02$ ) orientation [23]. The films were subsequently covered by a 10 nm thick Pd layer in order to prevent oxidation as well as to allow the catalytic uptake of H into the films, thus changing the amount of quenched disorder [24]. In the experiment, this was done by equilibrating the sample at a certain H pressure for one hour and then cooling down to 4.2K, where the experiments were carried out. During the cooling down process a phase separation of H-rich and H-poor regions sets in [25], where superconductivity is suppressed in the H-rich phase [26]. Thus the H-rich clusters of a size of roughly 0.1 to 1  $\mu\text{m}$  act as effective pinning sites for the vortices. We have varied the pinning density over a wide range by the use of a set of H loading pressures of 80, 260, 1130, and 1810 Pa. At these pressures, the resulting pinning density is such that the pinning sites can be treated as independent. The pinning density in the untreated sample, we estimate, corresponds to a pressure of roughly 10 Pa. For every H concentration, the field is increased in steps of 50  $\mu\text{T}$  from 0 to 20 mT, with an MO picture taken every step after letting the field relax for 3 seconds. This sequence is repeated twice, after zero field cooling the sample, in order to check for reproducibility [17].

As shown in Fig. 1, the magnetic field distribution changes drastically with the introduction of quenched disorder, leading to a more rugged and less compact landscape as the density of pinning centers is increased. Such a significant change has also been described for the shape and size distribution of the flux avalanches [17].

*Roughness analysis.* – In order to quantify the difference of the flux landscapes on increasing the density of H impurities, we have subsequently performed a roughness analysis of the magnetic field distributions [8,20]. A roughness analysis in both space and time can best be carried out by calculating the spatio-temporal correlation function of the flux landscape after subtracting the mean gradient, i.e. we consider  $b(x, y) = B_z(x, y) - \langle B_z(y) \rangle_x$ , where  $x$  ( $y$ ) is the coordinate parallel (perpendicular) to the mean vortex penetration direction. The correlation function is then defined by

$$C^2(x, y, t) = \langle (b(\xi + x, \eta + y, \tau + t) - b(\xi, \eta, \tau))^2 \rangle_{\xi, \eta, \tau}, \quad (1)$$

where  $\langle \cdot \rangle$  denotes an ensemble average. For a self-affine surface, the temporal correlation function scales as [20]  $C(0, t) \propto t^\beta$ , a power-law with an exponent  $\beta$ , called the growth exponent. The spatial part scales as  $C(r, 0) \propto r^\alpha$ , where  $\alpha$  is called the roughness exponent.

Here,  $r = \sqrt{x^2 + y^2}$  is the radial distance in the plane. In order to determine the full two dimensional (2d) roughness properties of the flux landscape, we determine the 2d correlation function in Fourier space using an FFT algorithm [8]. For this we determine the average position of the flux boundary by taking the point where the magnetic field strength is three times that of the standard deviation found in the Meissner state. From this position we go backwards towards the sample edge for 128 pixels, such that we have a square window of observation in the center of the sample. Subsequently, we perform a radial average of the spatial correlation function in order to determine the roughness exponent. Similarly, the growth exponent is determined. Due to the counting noise in the CCD camera, there is an intrinsic noise in the correlation function, which can strongly influence the determination of the roughness and growth exponents. We have previously characterised our system, such that we can determine the intrinsic noise precisely and correct for it [27]. In the following, we only show corrected correlation functions.

*Self-affine properties.* – The spatial part of the correlation function is shown in Fig.2 for the five different H concentrations. The curves are shifted by a factor of 1.5 for different amounts of impurities for clarity. As can be seen from the figure, in spite of the very different visual appearance of the flux landscape in Fig. 1, all of the curves follow the same power-law with an exponent of  $\alpha = 0.88(3)$ . This is in reasonable agreement with a determination of the

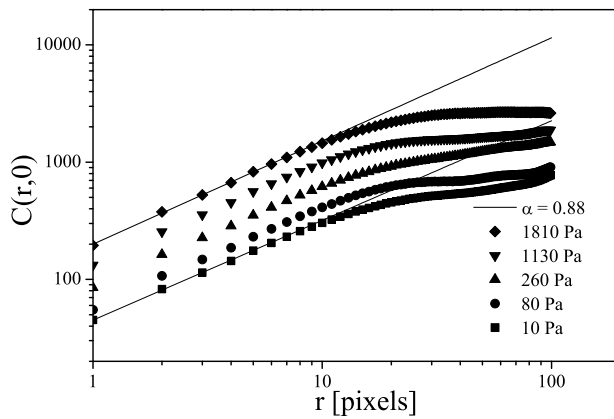


Fig. 2 – Radial average of the spatial correlation functions for different H loading pressures. The curves are shifted by a factor of 1.5 for different pressures for clarity. The correlation functions all follow a power-law with an exponent  $\alpha = 0.88(3)$  indicated by the solid line. This indicates that in spite of the different appearance of the flux landscapes on increasing the amount of quenched disorder, the roughness properties are unchanged. Thus a spatial scaling analysis cannot be used to characterise the appearance of SOC: we showed previously [17] that over this range of doping a transition from non-SOC to SOC behaviour takes place.

roughness of the flux *fronts* in an untreated Nb film by Vlasko-Vlasov *et al.* [4], however note that here we determined the exponents of the full *two dimensional flux landscape*. The rough flux front in combination with the fulfilment of a scaling relation between the fractal dimension and the roughness exponent was there taken as evidence for SOC [4]. Comparing our values

of the roughness exponent value with the fractal dimensions of the avalanches at different H concentrations discussed in [17] (decreasing from  $D = 2.75(5)$  for the untreated sample to  $D = 2.25(5)$  for high amounts of quenched disorder), we find the scaling relation  $D = d_B + \alpha$  to be fulfilled for all H. Here  $d_B$  is the fractal dimension of the avalanche area, which we determine using a boxcounting method and changes from  $d_B = 1.8(1)$  to  $d_B = 1.4(1)$  with increasing H concentration. Thus, despite the absence of SOC in part of the H-concentration range (as found from the avalanche behaviour [17]) we do find the same roughness exponent and fulfillment of the relation  $D = d_B + \alpha$  over the whole range. Hence these latter two criteria cannot be used to unequivocally decide that a system is SOC.

When looking at the temporal correlation functions shown in Fig. 3 however, one does observe a clear dependence of the growth exponent on the H concentration. In the untreated sample,  $\beta = 0.47(3)$ , whereas at higher H the value saturates at  $\beta = 0.80(3)$ . This clearly indicates that the differences between the SOC and non-SOC states can be seen in the dynamics of the flux landscape. As a matter of fact, determining the dynamic exponent, defined

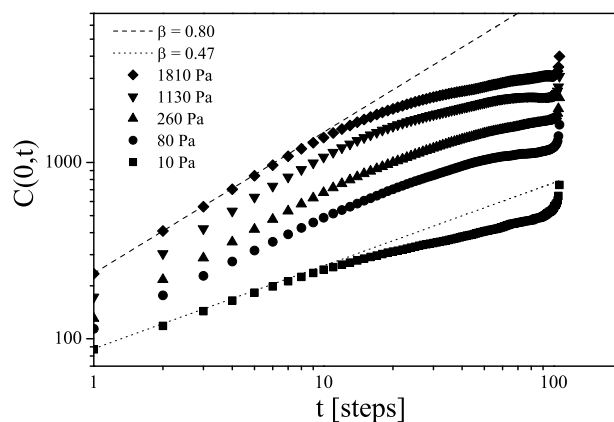


Fig. 3 – Temporal correlation functions for all of the different H loading pressures. The curves are shifted by a factor of 1.5 for different pressures for clarity. As can be seen, the exponent of the power-law increases from  $\beta = 0.47$  (dotted line) to  $\beta = 0.80$  (dashed line) with increasing disorder. This difference is due to the presence of a SOC state in the samples with higher disorder and hence a different dynamics of the flux landscape. This is corroborated by the levelling off of the dynamic exponent (Fig. 4) at the H loading pressures where finite size scaling of the avalanches is observed.

as  $z = \alpha/\beta$  [20] and shown in Fig. 4, one observes a leveling off of the value of  $z$  at higher H concentrations, where also finite size scaling and hence SOC is observed (see below). Furthermore, the asymptotic value is close to  $z = 1$ , which in directed percolation depinning (DPD) models corresponds to the critical state, i.e. the state at which the system is marginally stable [20, 28]. This shows that a determination of the dynamic exponent is essential to be able to conclude that a system is SOC from its roughness properties.

*Avalanche properties.* – The avalanche size distributions have been previously determined for different H concentrations. This has been achieved by taking difference images between two field steps and subsequently identifying the individual avalanches [17]. The magnetic flux change in each avalanche was determined from an integral of the change in  $B_z$  over

the area of the avalanche. From a finite size scaling collapse of the data, it was possible to determine values for the fractal dimension of the avalanches,  $D$ , and the avalanche size distribution exponent,  $\tau$ . In case there was no finite size scaling, these quantities could still be determined from the cut-off size and the distribution at small avalanche sizes respectively. Thus we have a dependence of the characteristic exponents with impurity density as well as a quality of the finite size scaling collapse. In Fig. 4, we also show the H dependence of the

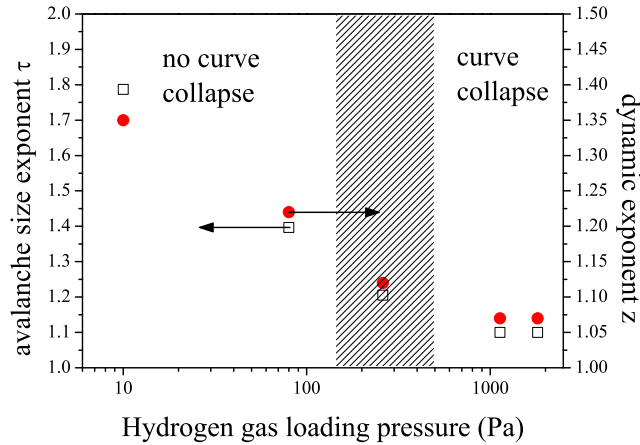


Fig. 4 – The avalanche size distribution exponent,  $\tau$ , (open squares) and the dynamic exponent,  $z$ , (full circles) as a function of H loading pressure. The value of the exponents decrease with increasing disorder. At low disorder, where no scaling collapse can be obtained, the avalanche exponent is obtained from a collapse at small avalanche size. The shaded region of H loading pressures gives the region where a scaling collapse becomes possible indicating the transition to SOC. This happens at the same H pressures where the avalanche exponent becomes 'universal' (i.e. independent of the amount of disorder) and the dynamic exponent levels off at a value close to 1, which is the value expected for the critical state in a DPD model.

avalanche size exponent. As can be seen from the figure, the exponent determined reaches its high disorder limit roughly at the point where good finite size scaling collapse is observed. Furthermore, it can be seen that the dynamic exponent saturates at the same values of the H pressure. This indicates that the transition to SOC can be determined from the value of the dynamic exponent  $z$  or from scaling collapse of the avalanche size distribution, but not from the roughness exponent  $\alpha$  alone.

*Conclusions.* – In conclusion, we have shown that the vortex landscape in H doped Nb films is self-affine with power-law scaling both in space and time. The spatial roughness is found to be independent of the H content of the sample, whereas the temporal roughness shows a marked H dependence. In combination with the fact that SOC as given by the finite size scaling collapse of the avalanche sizes can only be observed at higher levels of H induced disorder [17], this implies that the spatial roughness by itself cannot be used as a criterion for SOC. When studying the time correlation function however and therefore the dynamic exponent, a transition to a critical state with H doping can be observed. Comparing this finding with the characterisation of the avalanche size distributions, one finds that the

transition to finite size scaling collapse happens at the same H loading pressure as the leveling off of the dynamic exponent. Furthermore, the value at which the dynamic exponent levels off is that obtained in the DPD model for the critical point itself [20,28]. Thus we conclude that the presence of the SOC state can be inferred from a determination of the dynamic exponent as well as the finite size scaling of the avalanche size distribution.

*Acknowledgments.* – We would like to thank Ruud Westerwaal for help with the preparation of the samples. This work was supported by FOM (Stichting voor Fundamenteel Onderzoek der Materie), which is financially supported by NWO (Nederlandse Organisatie voor Wetenschappelijk Onderzoek).

## REFERENCES

- [1] BAK P., TANG C., AND WIESENFELD K., *Phys. Rev. Lett.*, **59** (1987) 381; *Phys. Rev. A*, **38** (1988) 364.
- [2] P. BAK, *How nature works* (Oxford Univ. Press) 1995; H.-J. JENSEN, *Self-Organized Criticality: Emergent Complex Behavior in Physical and Biological Systems* (Cambridge Univ. Press) 2000.
- [3] FIELD S., WITT J., AND NORI F., *Phys. Rev. Lett.*, **74** (1995) 1206; AEGERTER, C.M., *Phys. Rev. E*, **58** (1998) 1438; BEHNIA K., *et al.*, *Phys. Rev. B*, **61** (2000) R3815; ALTSHULER E., *et al.*, *Phys. Rev. B*, **70** (2004) R140505.
- [4] VLASKO-VLASOV V.K., *et al.*, *Phys. Rev. B*, **69** (2004) R140504.
- [5] PACZUSKI M., MASLOV S., AND BAK P., *Phys. Rev. E*, **53** (1996) 414;
- [6] AEGERTER C.M., GÜNTHER R., AND WIJNGAARDEN R.J., *Phys. Rev. E*, **67** (2003) 051306.
- [7] AEGERTER C.M., WELLING M.S., AND WIJNGAARDEN R.J., *Europhys. Lett.*, **65** (2004) 753.
- [8] AEGERTER C.M., WELLING M.S., AND WIJNGAARDEN R.J., *Physica A*, **347** (2005) 363.
- [9] JAEGER H.M., NAGEL S.R., AND BEHRINGER R.P., *Rev. Mod. Phys.*, **68** (1996) 1259; NAGEL S.R., *ibid.*, **64** (1992) 321 and references therein.
- [10] FRETTE V., *et al.*, *Nature, London*, **379** (1996) 49.
- [11] COSTELLO R.M., *et al.*, *Phys. Rev. E*, **67** (2003) 041304.
- [12] DICKMAN R., MUÑOZ M.A., VESPIGNANI A., AND ZAPPERI S., *Braz. J. Phys.*, **30** (2000) 27.
- [13] ALTSHULER E., *et al.*, *Phys. Rev. Lett.*, **86** (2001) 5490.
- [14] PACZUSKI M., MASLOV S., AND BAK P., *Europhys. Lett.*, **27** (1994) 97;
- [15] ALAVA M.J. AND LAURITSEN K.B., *Europhys. Lett.*, **53** (2001) 563; PRUESSNER G., *Phys. Rev. E*, **67** (2003) 030301.
- [16] VESPIGNANI A. AND ZAPPERI S., *Phys. Rev. Lett.*, **78** (1997) 4793; *Phys. Rev. E*, **57** (1998) 6345.
- [17] WELLING M.S., AEGERTER C.M., AND WIJNGAARDEN R.J., *Phys. Rev. B*, **71** (2005) 104515.
- [18] BLATTER G., *et al.*, *Rev. Mod. Phys.*, **66** (1995) 1125.
- [19] DE GENNES P.G., *Superconductivity of metals and alloys* (Addison-Wesley, New York) 1966.
- [20] BARÁBASI A.-L. AND STANLEY H.E., *Fractal Concepts in Surface Growth* (Cambridge University Press) 1995.
- [21] WIJNGAARDEN R.J., *et al.*, *Rev. Sci. Instrum.*, **72** (2001) 2661.
- [22] DOROSINSKII L.A., *et al.*, *Physica C*, **203** (1992) 149.
- [23] WELLING M.S., *et al.*, *Physica C*, **406** (2004) 100.
- [24] ALEFELD G. AND VÖLKL J., *Hydrogen in Metals II, Topics in applied Physics vol. 29* (Springer, Heidelberg) 1978.
- [25] SCHOBER T., *Phys. Stat. Solidi A*, **30** (1975) 107; NÖRTHEMANN K., KIRCHHEIM R., PUNDT A., *J. Alloys Comp.*, **356-357** (2003) 541.
- [26] MAKSIMOV E. G. AND PANKRATOV O. A., *Usp. Fiz. Nauk*, **116** (1975) 403; VINNIKOV L. YA. *et al.*, *Sov. J. Low Temp. Phys.*, **3** (1977) 4.
- [27] WELLING M.S., AEGERTER C.M., AND WIJNGAARDEN R.J., *Europhys. J. B*, **38** (2004) 93.
- [28] BARABÁSI A.-L., GRINSTEIN G., MUÑOZ M.A., *Phys. Rev. Lett.*, **76** (1996) 1481.